

Saving Energy with Relaxed Latency Constraints: A Study on Data Compression and Communication

Pietro Talli, *Student Member, IEEE*, Anup Mishra, *Member, IEEE*, Federico Chiariotti, *Senior Member, IEEE*, Israel Leyva-Mayorga, *Member, IEEE*, Andrea Zanella, *Senior Member, IEEE*, and Petar Popovski, *Fellow, IEEE*

Abstract—With the advent of edge computing, data generated by end devices can be pre-processed before transmission, possibly saving transmission time and energy. On the other hand, data processing itself incurs latency and energy consumption, depending on the complexity of the computing operations and the speed of the processor. The energy-latency-reliability profile resulting from the concatenation of pre-processing operations (specifically, data compression) and data transmission is particularly relevant in wireless communication services, whose requirements may change dramatically with the application domain. In this paper, we study this multi-dimensional optimization problem, introducing a simple model to investigate the tradeoff among end-to-end latency, reliability, and energy consumption when considering compression and communication operations in a constrained wireless device. We then study the Pareto fronts of the energy-latency trade-off, considering data compression ratio and device processing speed as key design variables. Our results show that the energy costs grows exponentially with the reduction of the end-to-end latency, so that considerable energy saving can be obtained by slightly relaxing the latency requirements of applications. These findings challenge conventional rigid communication latency targets, advocating instead for application-specific end-to-end latency budgets that account for computational and transmission overhead.

Index Terms—Latency, query age-of-information, energy consumption, computation and communication.

I. INTRODUCTION

Sensor-based wireless data collection is an essential service of modern communication networks, supporting an ever-widening set of applications, from long-term environmental monitoring to virtual reality and industrial automation [1], [2]. Notably, as the variety of sensing scenarios expands, sensor nodes evolve to incorporate enhanced computing capabilities. These capabilities can be leveraged to compress the sensed data before transmission, potentially reducing delay and energy costs of transmission. On the other hand, data processing itself incurs costs in terms of delay and energy consumption.

P. Talli (corresponding author – pietro.talli@phd.unipd.it), F. Chiariotti (federico.chiariotti@unipd.it), and A. Zanella (andrea.zanella@unipd.it) are with the Department of Information Engineering, University of Padova, Italy. A. Mishra (anmi@es.aau.dk), I. Leyva-Mayorga (ilm@es.aau.dk), and P. Popovski (petarp@es.aau.dk) are with the Department of Electronic Systems, Aalborg University, Denmark. This work was supported by the European Union under the Italian National Recovery and Resilience Plan of NextGenerationEU, under the partnership on “Telecommunications of the Future” (PE0000001 - program “RESTART”) and, in part, by the Velux Foundation, Denmark, through the Villum Investigator Grant WATER, nr. 37793. Anup Mishra is supported by the Horizon Europe Marie Skłodowska-Curie Actions (MSCA) Postdoctoral Fellowships under the project FOCUS-6G (Grant Agreement No. 101202623).

Therefore, the typical key performance indicators (KPIs) of wireless networks, namely latency, reliability, and energy efficiency (EE), are jointly influenced by decisions made in both computation and communication stages [3]–[6].

Higher (lossless) compression ratios generally require more processing cycles and, consequently, longer processing time. This can be reduced by increasing the processing speed, at the cost of a higher computing power. On the other hand, compression reduces the amount of data to be transmitted, thus saving transmission time and potentially energy for a certain level of reliability [7]. In parallel, communication time can be significantly reduced by increasing the transmission data rate. However, under a fixed bandwidth, this approach requires higher transmission power to reach a signal-to-noise ratio (SNR) sufficient to ensure reliable data transmission despite the increased speed.

While the general trade-offs between energy, latency and reliability are well known at the level of individual operations [3], [6], [8], their interplay becomes more nuanced in the context of an end-to-end chain of operations within a wireless sensor network possessing computational capabilities. This complexity arises from the coupled effects of compression and transmission decisions: while increasing the compression ratio makes transmission faster and more efficient, it also has a computational cost that affects both the latency and the sensor’s energy budget. Consequently, there is a growing need for improved modeling and understanding of the interplay between system design parameters and device-level constraints. By simultaneously modeling computation and communication, we can gain deeper insights into optimal resource allocation strategies. This approach enables us to better balance and optimize energy consumption, latency, and reliability across the entire system. Such comprehensive modeling is particularly relevant as we progress towards more complex and integrated network architectures in future wireless communication systems. It provides a foundation for developing more efficient, adaptive, and resilient networks that can meet the diverse demands of emerging applications and technologies.

A. Contributions

In this paper, we present a model that enables the exploration of the Pareto region between latency and energy consumption for a fixed reliability level in a joint computation-communication setting. We focus on lossless compression, so that the fidelity of the reconstructed data is preserved, and accuracy is not a concern. By treating the data compression ratio

and processing speed as design variables, we identify system operating points and demonstrate that modest relaxations in latency requirements can lead to substantial energy savings. Leveraging modeling approximations developed in our prior works [9], [10], we extend the analysis of joint computation–communication scenarios by explicitly accounting for the energy costs of both computation and communication across varying reliability levels. This provides a more comprehensive perspective on system-level energy–latency optimization, which covers a gap in the current literature, as discussed in the next section.

To this end, we consider an open-loop system where a sensor transmits uplink data to the base station (BS). The computational aspect involves compression at the sensor and decompression at the BS. We present an analytical model to examine the interplay of the two operations in terms of the trade-off between latency and energy consumption across two target scenarios.

- (i) *Power-constrained scenario*, we build on the statistical latency modeling approach from [9] to characterize the end-to-end latency and optimize it under a given energy budget.
- (ii) *Time-constrained scenario*, reflects a scheduled access where each sensor is assigned a fixed time slot for compression and communication, such as to deliver the data at a specific instant as requested by a query. The data is sampled at the start of the fixed time slot, such that the slot duration corresponds to query age-of-information (QoI) [11]. Here, we optimize energy consumption subject to a target reliability constraint [11].

The major contribution of this paper are the following:

- We define an open-loop uplink system model to investigate the energy–latency trade-off in a joint computation–communication scenario. The model captures compression at the sensor, decompression at the BS, and packet-based transmission with reliability constraints, enabling a unified analysis of processing and communication operations.
- We develop an analytical framework to model both compression and transmission processes in terms of energy and latency. Compression is parameterized by the compression ratio and processing speed, while the transmission model captures the impact of compression on packet count and retransmissions. Both components are characterized statistically, allowing us to evaluate not only expected values but also variability and worst-case performance through latency quantiles.
- We formulate a power-constrained optimization problem, where the goal is to minimize the ρ -quantile of the end-to-end latency under a total energy budget. For tractability, we derive an upper bound on the latency quantile and prove convexity of the relaxed problem under mild conditions. We show that the problem can be efficiently solved by performing a binary search over the compression ratio.
- We formulate a complementary time-constrained optimization problem, relevant for scheduled access scenarios

governed by QoI constraints. In this setting, we minimize energy consumption while meeting a fixed QoI budget and target reliability. We derive the optimal allocation of compression time and transmission time to jointly satisfy these constraints.

- Through Pareto front analysis, we quantify the trade-offs between latency and energy consumption across varying reliability levels. Our results show that modest relaxations in latency constraints can lead to substantial energy savings. We also demonstrate how system-level parameters, such as compression ratio and processing speed, can be jointly tuned to optimize both latency and energy consumption under different operational constraints.

B. Organization

The paper is organized as follows. Sec. II provides a quick overview of the state of the art of energy-latency and reliability analysis in wireless networks, highlighting the gaps covered by this work. Sec. III provides detailed explanations of the analytical models for compression, decompression, and transmission that we use throughout the paper. In Sec. IV we describe and analyze the two considered scenarios. For each of them, we provide an analytical characterization of the latency, energy consumption and reliability. Moreover, we define an optimization problem and discuss solutions and optimization strategies. Sec. V then presents the results of simulations with realistic parameters, which show how the proposed trade-offs can arise in real-world devices and networks. Finally, Sec. VI summarizes the key findings and proposing potential directions for future research.

II. RELATED WORK

This work builds on the well-known trade-off between source coding and channel coding [12], [13]. In the context of communication systems, the energy–latency trade-off has received considerable attention in the literature [8], [14], [15]. For example, [14] investigates the delay and power consumption trade-off incorporating buffer constraints. In [8], the authors explore energy-latency trade-offs in ultra reliable low latency communication (URLLC) systems by optimizing retransmissions and blocklength. Similarly, [15] develops a scheduling algorithm grounded in finite blocklength theory and derives energy–delay bounds.

Energy–latency trade-offs have also been examined in the context of compression operations [16]–[18]; however, since our primary focus is on the communication stage, we do not discuss these works in detail here. Finally, in regards to joint computation-communication systems, the trade-off has been primarily investigated in the context of edge task offloading [3], [4], [9], [10], [19], [20]. The work [9] focused on the statistical modeling of end-to-end latency, while [4] addressed energy optimization across processing and communication components. Reference [19] theoretically explores the trade-off between computation load and communication load through data reduction functions. Similarly, [20] jointly optimizes computation and communication for real-time monitoring of dynamic systems. More recently, [10] proposes a

unified statistical framework for modeling both computation and communication. The authors focus on a rigorous characterization of end-to-end latency in Goal-oriented Communication (GoC) context, where delays arise from compression, processing, and transmission. Latency is optimized with respect to multiple design parameters, providing a holistic view of timing in distributed systems.

In summary, most of existing works in the literature are constrained to predefined latency-reliability requirements, without much flexibility for the actual timing requirements of the applications [21]. Moreover, in many network scenarios, it remains an open question whether it is more beneficial to invest energy in compressing data sources to reduce communication overhead, or to allocate more energy to channel coding to enhance reliability [5], [10]. Hence, a significant gap exists in current research regarding the trade-offs between latency-reliability guarantees and energy consumption, especially in scenarios where devices can process and reduce data size through methods like compression.

A. Notation

Matrices are denoted by boldface uppercase letters, column vectors are denoted by boldface lowercase letters, and scalars are denoted by standard letters. $\mathbb{E}_X[Y]$ denotes the expectation of Y with respect to the random variable X . $\mathbb{C}^{M \times N}$ and $\mathbb{R}^{M \times N}$ denote the sets of all $M \times N$ matrices with complex- and real-valued entries, respectively. The circularly symmetric complex Gaussian (CSCG) distribution with mean μ and variance σ^2 is denoted by $\mathcal{CN}(\mu, \sigma^2)$. The Big-O notation $\mathcal{O}(f(n))$ describes the asymptotic upper bound of an algorithm's computational complexity. The floor and ceiling functions are denoted by $\lfloor x \rfloor$ and $\lceil x \rceil$, representing the greatest integer less than or equal to x and the smallest integer greater than or equal to x , respectively.

III. SYSTEM MODEL

In this section, we present the energy and latency models for an open-loop system, where a wireless sensor is transmitting uplink data to the BS. We define a *Computational Model* which entails the compression at the sensor and decompression at the BS, and a *Communication model* that captures the data transmission over the wireless channel. We characterize each model in terms of latency and energy requirements, and then analyze their joint optimization in the following section.

A. Computational Model

For analytical simplicity, we focus on lossless compression in this work.¹ The compression ratio $Q \in [1, Q_{\max}]$ is defined as the ratio between the size of the original data block and the size of the corresponding compressed output. The maximum value Q_{\max} corresponds to the maximum possible data reduction in lossless compression.

¹Incorporating lossy compression would introduce the additional dimension of accuracy. This will be explored in future work to examine the trade-offs between energy, latency, reliability, and accuracy.

Common lossless compression algorithms use dictionary-based methods such as Lempel-Ziv [22], which require scanning through the content multiple times to further reduce the output size. Therefore, larger compression ratios generally require a greater computational effort [23]. Quantitatively, computational complexity can be expressed in terms of number of required cycles of the central processing unit (CPU) for bit of processed data. This number can be modeled as a Gamma-distributed random variable $X_c \sim \text{Gamma}(\kappa, \beta)$, characterized by its shape parameter κ and scale parameter β [24], [25]. Following [23], the relation between the compression ratio Q and the mean computational complexity $\mathbb{E}[X_c]$ can be modeled as:

$$\mathbb{E}[X_c] = e^{\psi Q} - e^{\psi}, \quad (1)$$

where $\psi > 0$ is a constant that depends on the compression algorithm used [23], [26]. From (1), it can be discerned that the expected number of operations increases exponentially with Q .

The compression time T_c for a data block of D bits is directly proportional to X_c , and can be expressed as [3]:

$$T_c = \frac{X_c D}{f_c}, \quad (2)$$

where f_c is the CPU-cycle frequency of the device [23]. From (1) and (2), it follows that $T_c \sim \text{Gamma}(\kappa, \beta D f_c^{-1})$.

The number of operations X_d necessary for decompression is generally lower than X_c and can be modeled as a deterministic fraction $\zeta \in (0, 1]$ of X_c [27]–[29]. We also note that decompression is performed at the BS, which typically operates under less stringent energy constraints and has greater computational capacity, further decreasing the impact of T_d on the overall latency.

The CPU-cycle frequency f_c also affects the average power consumed during the compression operation. In fact, according to [4], [18], the power absorbed per CPU-cycle grows cubically with the CPU clock. Therefore, denoting by $P_{s,\max}$ the maximum processing power at the sensor, and by $f_{c,\max}$ the maximum CPU-cycle frequency, the average power consumed per CPU cycle can be estimated as [4]:

$$P_c(f_c) = P_{s,\max} \left(\frac{f_c}{f_{c,\max}} \right)^3. \quad (3)$$

Using (3), the average energy consumption for the compression operation can be calculated as [9]:

$$E_c(f_c, Q) = P_c(f_c) \mathbb{E}[T_c] = P_{s,\max} \frac{(e^{\psi Q} - e^{\psi}) D f_c^2}{(f_{c,\max})^3}. \quad (4)$$

The energy for decompression at the BS depends on its processing power, but follows the same model.

B. Communication model

We consider a linear communication channel model, where the channel is represented by parameter $h \in \mathbb{C}$, which follows a Rayleigh block fading model. The channel gain $g = |h|^2$ is then exponentially distributed, i.e., $g \sim \text{Exp}(1)$ [30]. We denote the uplink transmission power as P_{tx} and bandwidth as B . Within a block, the transmitted data packet is correctly

decoded only if the SNR at the BS exceeds a threshold γ_{th} . By virtue of the block fading assumption, the SNR remains the same for the whole packet and the channel realization is independent for each packet [30]. The SNR at the BS for a transmitted packet can be expressed as [9]:

$$\gamma(P_{\text{tx}}, B, d) = \frac{K_0 P_{\text{tx}}}{d^\ell N_0 B} g = \gamma_0(P_{\text{tx}}, B, d) g, \quad (5)$$

where K_0 is the Friis equation parameter, ℓ is the path loss exponent, N_0 is the noise power spectral density, d is the sensor-BS distance, and γ_0 is the average SNR [9], [30]. Given (5), the outage probability with respect to a target SNR γ_{th} can be calculated as:

$$\varepsilon = \Pr[\gamma < \gamma_{\text{th}}] = \Pr[g < \gamma_{\text{th}}/\gamma_0] = 1 - e^{-\frac{\gamma_{\text{th}}}{\gamma_0}}. \quad (6)$$

The Shannon outage rate is $R(\varepsilon) = B \log_2(1 + \gamma_{\text{th}})$, with $\gamma_{\text{th}} = -\gamma_0 \ln(1 - \varepsilon)$. Consequently, the time required to transmit a packet of n_p bits is given by [9]:

$$t_p = n_p / R(\varepsilon). \quad (7)$$

We consider a persistent automatic repeat request (ARQ) scheme, wherein a packet is automatically retransmitted until it is correctly decoded and acknowledged by the receiver. For simplicity, we assume an ideal feedback channel. This assumption does not compromise the accuracy of our latency-energy model, as potential downlink errors could be accounted for in the link budget of the uplink transmission.

Subsequently, we consider the standard definition of EE η given in [31] as:

$$\eta [\text{bit/Joule}] = \frac{\text{Payload data rate} [\text{bit/s}]}{\text{Power consumption} [\text{Joule/s}]}. \quad (8)$$

Note that, the denominator of (8) accounts for both the transmission power and circuit power [31] that, in turn, accounts for the power consumption of the analog-to-digital converter (ADC) for sampling at a given bandwidth B , as well as the power required for the channel encoding and decoding processes. While the former can be expressed as νB , the latter is proportional to the data rate and can be calculated as $\lambda R(\varepsilon)$ [31]. Both ν and λ are hardware-specific parameters. We then obtain the EE as:

$$\eta(\varepsilon) = \frac{R(\varepsilon)}{P_{\text{tx}} + \nu B + \lambda R(\varepsilon)}. \quad (9)$$

We use (9) in the following section to compute the power required for data transmission in the respective target scenarios, from which we can obtain the energy consumed during the transmission step.

IV. OPTIMIZATION UNDER RESOURCE CONSTRAINTS

In this section, we analyze two representative resource-constrained scenarios typical of sensor-based wireless systems and compute their overall latency and energy consumption for varying reliability levels. Subsequently, by treating the compression ratio Q and processing speed f_c as design variables, we derive the Pareto front for the energy-latency trade-off in both scenarios. Note that, as many applications are sensible to latency peaks, rather than average values, we

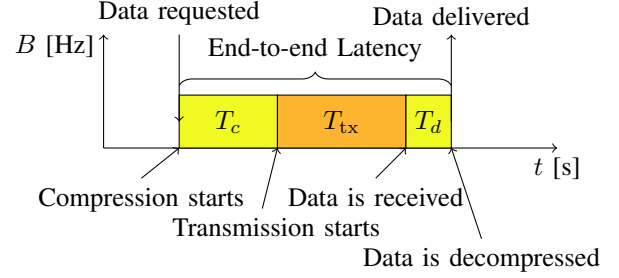


Fig. 1. Power-Constrained scenario.

consider the ϱ -quantile of the latency, as we are interested in worst-case performance. Conversely, we only consider average energy consumption, as batteries smooth out the instantaneous variations in used energy and, therefore, performance only depends on the mean value.

A. Power-Constrained Scenario

In this scenario, the sensor is allocated a dedicated wireless channel with bandwidth B and transmits without scheduling delays or resource contention. The transmit power is then fixed and equal to P_{tx} . Consequently, the energy allocated per transmitted bit is obtained using (9). We assume a message is compressed and immediately transmitted. The end-to-end latency, denoted by T , is then given by the sum of compression, transmission, and decompression times, as illustrated in Fig. 1. Our objective is to determine the optimal parameter configurations $\{f_c, Q\}$ to minimize the ϱ -quantile of the latency [9], for a given energy budget E_{max} .

Formally, denoting by $F_T(t) = \Pr[T \leq t]$ the cumulative distribution function (CDF) of T , the resulting optimization problem can then be expressed as:

$$\begin{aligned} \min_{f_c, Q} \quad & F_T^{-1}(\varrho), \\ \text{s.t.} \quad & E(f_c, Q) \leq E_{\text{max}}, \end{aligned} \quad (\text{P1})$$

where the objective function is the ϱ -quantile of end-to-end latency T . In the following, we will show that (P1) can be efficiently solved via a binary search over the optimization variable Q .

1) *Timing*: Let us consider a data block of D bits, whose compression time T_c is obtained from equation (2). After compression, the $\lceil D/Q \rceil$ bits are segmented into packets of equal length n_p , with padding applied as needed to obtain an integer number N of packets, with

$$N = \left\lceil \frac{D}{Q n_p} \right\rceil. \quad (10)$$

As channel realizations for subsequent packets are independent and identically distributed due to the block fading assumption, the number of attempts necessary to transmit a single packet follows a geometric distribution with parameter $1 - \varepsilon$ [9]. Accordingly, the probability of requiring exactly K attempts to correctly receive a packet is given by:

$$\Pr[K = k] = \varepsilon^{k-1} (1 - \varepsilon), \quad k \geq 1, \quad (11)$$

Consequently, the time required to successfully transmit one packet, denoted by \mathcal{T} , is a random variable with the same

distribution as K , scaled by the transmission time t_p . The expected value and variance of variable \mathcal{T} are expressed as:

$$\begin{aligned}\mathbb{E}[\mathcal{T}] &= \frac{1}{(1-\varepsilon)}t_p, \\ \mathbb{E}[(\mathcal{T} - \mathbb{E}[\mathcal{T}])^2] &= \frac{\varepsilon}{(1-\varepsilon)^2}t_p.\end{aligned}\quad (12)$$

Following equations (7) and (12), the total transmission time for a data block of N packets is given by:

$$T_{\text{tx}} = \sum_{i=1}^N \mathcal{T}_i \quad (13)$$

where the \mathcal{T}_i are independent and identically distributed (i.i.d) random variables, with geometric distribution. Equivalently, the total number of transmission attempts, N_{tx} , follows a negative binomial distribution with parameters $\{N, \varepsilon\}$, representing the number of trials needed to achieve N successful packet deliveries. The total transmission time, therefore, follows the same distribution as N_{tx} , scaled by the packet duration t_p :

$$T_{\text{tx}} = N_{\text{tx}} \cdot t_p. \quad (14)$$

Consequently, the end-to-end latency, T , is calculated as:

$$T = T_c + T_{\text{tx}} + T_d = \left(1 + \frac{\zeta f_c}{f_b}\right) T_c + T_{\text{tx}}, \quad (15)$$

where we assumed $T_d = \frac{\zeta f_c}{f_b} T_c$, with f_b denoting the BS CPU frequency. The end-to-end latency random variable, T , is thus obtained as the sum of two components: a scaled version of T_c , which is modeled as a Gamma-distributed random variable, and T_{tx} , which follows a negative binomial distribution scaled by the duration t_p . As a result, the distribution of T is not available in closed form and must be characterized numerically or through approximation techniques. To this end, a recent work [10] investigated Saddle Point Approximation (SPA) to obtain the CDF of the sum of random variables describing different latency components in a more general case. However, we can exploit our knowledge of the distributions of the various components to propose a more tractable upper bound and provide reliability guarantees on the end-to-end latency T . Following [10], we observe that for $N \gg 1$ and sufficiently small t_p , the time T_{tx} can be approximated by a Gaussian distribution as:

$$\mathcal{N}\left(\mu_{\text{tx}} = \frac{Nt_p}{(1-\varepsilon)}, \sigma_{\text{tx}}^2 = \frac{Nt_p^2\varepsilon}{(1-\varepsilon)^2}\right). \quad (16)$$

As a consequence, the end-to-end latency can be approximated as $T \simeq (1 + (\zeta f_c/f_b)) T_c + T_{\text{tx}}^G$, where $T_{\text{tx}}^G \sim \mathcal{N}(\mu_{\text{tx}}, \sigma_{\text{tx}}^2)$.

2) *Energy*: Similar to the end-to-end latency, the system's overall average energy consumption E is given by the sum of the computation and communication energy:

$$E = E_c + E_{\text{tx}} = P(f_c)\mathbb{E}[T_c] + E_{\text{tx}}. \quad (17)$$

Here, we omitted the decompression energy, as it does not affect the transmitter's battery life: the BS is assumed to be connected to a power source, and is thus irrelevant to our study. The compression energy E_c can be easily computed

following the discussion in Section III-A. On the other hand, the communication energy is:

$$E_{\text{tx}} = \frac{n_p \mathbb{E}[T_{\text{tx}}]}{\eta(\varepsilon)t_p}, \quad (18)$$

as the energy required to transmit a single packet is $n_p/\eta(\varepsilon)$.

3) *Optimization*: In the following, we find an approximate solution to problem (P1). We first express the energy constraint in problem (P1) as an explicit function of f_c and Q :

$$\frac{(e^{\psi Q} - e^{\psi})DP_{s,\max}f_c^2}{f_{\max}^3} + \frac{D}{(1-\varepsilon)Q\eta(\varepsilon)} \leq E_{\max}. \quad (19)$$

Then, we express the average number of transmitted packets, including retransmissions, as $N/(Q(1-\varepsilon))$, omitting the ceiling operation for better tractability. The following lemma can then be obtained by analyzing the behavior of the utility function and the constraint in (19) with respect to f_c .

Lemma 1. *For any optimal pair (f_c^*, Q^*) , the constraint in (19) is always satisfied with equality leading to the following relationship between f_c^* and Q*

$$f_c^* = \sqrt{\frac{E_{\max} - \frac{D}{(1-\varepsilon)Q\eta(\varepsilon)}}{(e^{\psi Q} - e^{\psi})DP_{s,\max}/f_{\max}^3}}. \quad (20)$$

Proof. As the computation frequency f_c increases, the computation time monotonically decreases, and thus the overall latency decreases. Since the computation time follows a Gamma distribution, scaled by the inverse of the frequency, we can easily prove that $\forall f_{c,1} > f_{c,2}$ and $\forall \varrho$, it holds $F_{T_c}^{-1}(\varrho, f_{c,1}) < F_{T_c}^{-1}(\varrho, f_{c,2})$, i.e., the computation time using $f_{c,2}$ has first order stochastic dominance with respect to $f_{c,1}$. By definition, any quantile ϱ of the computation latency distribution is then a monotonically decreasing function of f_c , and the condition is extended to strict monotonicity if $Q > 1$. As the communication latency for a fixed Q is independent of f_c , this also holds for the overall latency. On the other hand, the energy increases monotonically (quadratically) as f_c increases. It then follows that choosing the highest possible computation frequency, i.e., satisfying the constraint at equality, is optimal for any set value of Q^* . Setting (19) as an equality and solving for f_c , we obtain (20), which concludes the proof.

Using (20), problem (P1) can be rewritten as an optimization problem with a single variable, Q . However, the end-to-end latency remains intractable, as it is the sum of a Gamma-distributed and a Gaussian-distributed random variable, both of which are functions of the compression parameter Q . We then solve the problem for a tractable upper bound for the ϱ -quantile of the latency distribution, denoted by $F_T^{-1}(\varrho)$.

Lemma 2. *The ϱ -quantile of the sum of a Gamma and a Gaussian random variable is upper-bounded by the sum of the quantiles of the two components,*

$$F_T^{-1}(\varrho) \leq F_{T_c}^{-1}(\varrho) + F_{T_{\text{tx}}}^{-1}(\varrho). \quad (21)$$

Proof. This result follows as a special case of a more general bound presented in [9]. The key property invoked to prove the lemma is the sub-additivity of the quantile function for

unimodal log-concave distributions [32]. These properties hold for both the Gamma and Gaussian distributions.

The result allows to relax the optimization problem in (P1) to the minimization of an upper-bound of the latency with respect to Q . The relaxed problem is formulated as:

$$\min_Q F_{T_c}^{-1}(\varrho, Q, f_c^*(Q)) + F_{T_{tx}}^{-1}(\varrho, Q, f_c^*(Q)), \quad (P2)$$

where Lemma 1 is used to express the optimal compression frequency f_c^* as a function of Q , and Lemma 2 is applied to upper-bound the ϱ -quantile of the end-to-end latency by the sum of the corresponding quantiles of the compression and transmission components. Subsequently, we investigate the convexity of problem (P2) with respect to Q .

Theorem 1. *Problem (P2) is convex with respect to Q , under the condition*

$$Q^2 3\psi^2 e^\psi - 2QE_{\max} + \frac{D}{(1-\varepsilon)\eta(\varepsilon)} \geq 0. \quad (22)$$

Proof. To prove that the unconstrained problem is convex, it suffices to show that both quantiles are convex with respect to Q . The statement of the theorem then trivially follows, given that the sum of two convex functions is itself convex. The condition in (22) ensures the convexity of the quantile function associated with the Gamma-distributed compression time; a detailed analytical derivation of this condition is provided in Appendix A. On the other hand, the quantile function of the Gaussian-distributed compression time can be written as $F_{T_{tx}}^{-1}(\varrho) = \mu_{tx} + z(\varrho)\sigma_{tx}$, where $z(\varrho)$ is the probit function, i.e., the inverse CDF of the standard normal distribution. Substituting the expressions for μ_{tx} and σ_{tx} , we obtain:

$$F_{T_{tx}}^{-1}(\varrho) = \frac{Nt_p}{1-\varepsilon} + z(\varrho) \cdot t_p \cdot \sqrt{\frac{\varepsilon N}{(1-\varepsilon)^2}}. \quad (23)$$

Since $N = \frac{D}{Qn_p}$ is a non-increasing and convex function of Q for $Q > 0$, and both the mean and standard deviation of the Gaussian distribution are affine in N , it follows that $F_{T_{tx}}^{-1}(\varrho)$ is convex in Q :

$$F_{T_{tx}}^{-1}(\varrho) = z(\varrho) \frac{Dt_p^2 \varepsilon}{Qn_p(1-\varepsilon)^2} + \frac{Dt_p}{Qn_p(1-\varepsilon)}. \quad (24)$$

Since $F_{T_{tx}}^{-1}(\varrho)$ is the sum of two functions, each of which is convex in Q for $Q > 0$, it is itself a convex function of Q , which concludes the proof.

Although we proved that the problem is convex under reasonable conditions, we could not derive a closed-form expression for the minimum latency. However, the optimization problem in the power-constrained scenario can be efficiently solved using a binary search algorithm, with computational complexity $O\left(\log\left(\frac{Q_{\max}-1}{\theta}\right)\right)$, where θ is the desired precision of the solution. Alternatively, the problem can be tackled using Lagrangian methods or other standard convex optimization solvers.

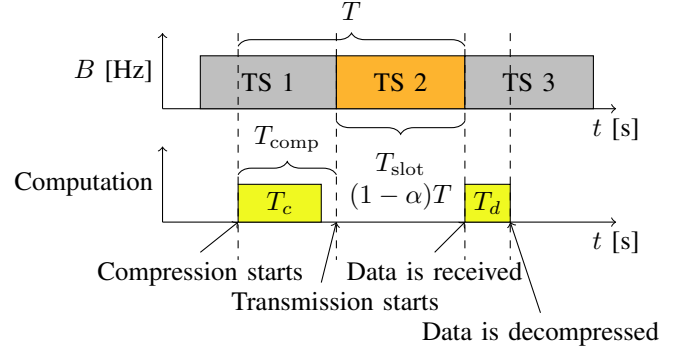


Fig. 2. Time-Constrained scenario.

B. Time-Constrained Scenario

In this second target scenario, we change the access model by dividing the channel into time-frequency slots. The objective is to design a system that ensures the total time for compression and transmission does not exceed a fixed maximum duration T in order to meet QoI requirements. Note that we are not explicitly modeling the reception and processing of the query. Its impact is operationalized by: (1) setting a specific time instant by which the transmission should be finalized; and (2) predefined value of how aged the information delivered at that instant should be, which is the QoI. Compression and communication must each occur within pre-allocated time slots. This model could be used in scenarios where multiple sensors are assigned in advance some communication resources to transmit their data, so that all transmissions are scheduled and occur without risk of mutual interference. This approach can also enhance EE in compression, as each sensor can utilize the waiting time before its scheduled transmission slot to compress the data, balancing the computational load.

The QoI here spans across three time slots: the transmission slot, used to send the compressed data, and the slot before and after that, which are used to compress and decompress data before and after transmission, respectively. An illustrative example is shown in Fig. 2, where it is assumed that the data is sampled just at the instant when the compression starts. While in the Power-constrained scenario the energy budget, which was our constraint, could be optimally divided between the compression and communication operations, here the time constraint T must necessarily fall within the compression and communication slots, which are predefined. However, within these boundaries, we can still adjust the compression time to maximize the overall EE. We then introduce an additional optimization variable $\alpha \in [0, 1]$, such that $T_{\text{comp}} = \alpha T$ is the fraction of time allocated for compression, while $T_{\text{comm}} = (1 - \alpha)T$ is the communication slot. Note that we consider only the compression time in the optimization, as the decompression time is negligible in comparison. Furthermore, given the computing capabilities at the BS, it can be assumed that decompression is always completed within the allocated slot whenever the data is successfully compressed and transmitted. As a consequence, while T is not strictly equal to the QoI, it is equivalent in this context. The probability that the compression and transmission

processes are not successfully completed within the allocated time are indicated as ε_c and ε_{tx} , respectively. Considering that these operations are independent, the overall reliability of the communication can then be expressed as the product of the success probabilities of the compression and transmission steps, that is $P_{succ} = (1 - \varepsilon_c)(1 - \varepsilon_{tx})$. The constraint in this target scenario is that we need to ensure that the system reliability is at least ϱ . The goal of the optimization problem is then to minimize the average energy consumption for the chosen reliability:

$$\begin{aligned} \min_{f_c, Q, \alpha} \quad & E_c(f_c, Q) + E_{tx}(P_{tx}, Q), \\ \text{s.t.} \quad & F_{T_c}(T_{comp}) \geq 1 - \varepsilon_c, \\ & F_{T_{tx}}(T_{comm}) \geq 1 - \varepsilon_{tx}, \\ & (1 - \varepsilon_c)(1 - \varepsilon_{tx}) \geq \varrho. \end{aligned} \quad (\text{P3})$$

1) *Timing*: As shown in Fig. 2, the compression operation must terminate before the transmission begins, i.e., $T_c < T_{comp}$. This sets the first constraint of the system, requiring data to be reliably compressed before the start of the assigned time-frequency slot. Fixing Q and f_c implicitly leads to a fixed contribution to the QAOI, provided that the operation concludes in time. The overall time between the beginning of compression at the transmitter and the decoding of the data at the receiver is the QAOI [11], as it represents the freshness of the information available to the receiver if the time slot allocation aligns with client requests. The QAOI is hence expressed as:

$$\text{QAOI} = T_{comp} + T_{comm} + T_{d,max}, \quad (25)$$

where $T_{d,max}$ is the time allocated for decompression which can be computed as:

$$T_{d,max} = T_{comp} \frac{f_{c,max}}{f_b}. \quad (26)$$

Since the sampling and transmission instants are predetermined by virtue of allocation of the respective slots, compression must happen within T_{comp} , or the sensor will be unable to transmit in the transmission slot T_{comm} . In this case, the transmitter receives a feedback on the success of transmitted packets only after the slot terminates and, consequently, it cannot rely on retransmissions. As such, we propose packet-level coding to reduce the message error probability. Efficient packet-level codes enable decoding of a block of N original packets if at least N out of the $N_{tx} > N$ transmitted packets are correctly received [33]. Assuming a Bernoulli error process, the transmission error probability is obtained as:

$$\varepsilon_{tx} = \sum_{h=0}^{N-1} \binom{N_{tx}}{h} (1 - \varepsilon)^h \varepsilon^{N_{tx}-h}, \quad (27)$$

where ε is the channel packet error probability. Building on this, the resulting QAOI is a constant as problem (P3) is optimized to restrict both compression and communication with a predetermined time interval.

2) *Energy*: Sec. III-A models the compression time as a Gamma distribution. In this scenario, however, we assume that the compression procedure is forced to terminate, even if incomplete, at the beginning of the transmission slot. This results in a distribution of the compression time that is a

truncated Gamma distribution. The energy for compression E_c is then computed as

$$E_c = ((1 - \varepsilon_c)\mathbb{E}[T_c | T_c < T_{comp}] + \varepsilon_c T_{comp}) P_c(f_c). \quad (28)$$

The expected value of the truncated Gamma distribution admits a closed-form solution [34]. In the following, we derive this solution with respect to the parameters considered here as:

$$\mathbb{E}[T_c | T_c < T_{comp}] = \frac{\beta D}{f_c} \frac{\gamma(\kappa + 1, \frac{\beta D}{f_c T_{comp}})}{\gamma(\kappa, \frac{\beta D}{f_c T_{comp}})} = \bar{T}_c^{\text{trunc}}, \quad (29)$$

where $\gamma(s, x) = \int_0^x t^{s-1} e^{-t} dt$ is the lower incomplete gamma function and $\beta = (e^{\psi Q} - e^{\psi})/\kappa$. It follows that the average energy consumption for compression is given by $E_c(f_c, Q) = P(f_c) \bar{T}_c^{\text{trunc}}$. On the other hand, since retransmissions are not employed, the number of transmitted packets is fixed as:

$$N_{tx} = \left\lfloor \frac{(1 - \alpha)T}{t_p} \right\rfloor. \quad (30)$$

Therefore, the communication slot, T_{comm} , is fully utilized to maximize reliability. The communication energy is then determined by (18).

3) *Optimization*: Similar to (P1), problem (P3) can be solved for a given QAOI, with f_c , Q and α as optimization variables. In this case we can note that, for any pair (Q, α) , we can always decrease the processing frequency f_c until the constraint on overall reliability is strict, i.e., satisfied with equality. The proof is complementary to Lemma 1, as both the compression energy E_c and the probability of successful compression $(1 - \varepsilon_c)$ decrease monotonically as f_c increases.

On the other hand, the utility function and the constraint in (P3) are not monotonic in Q and α , preventing further simplification of the optimization procedure. The optimization problem is not convex and is solved through exhaustive search on the parameter space. However, given a pair (α, Q) , it is still possible to perform binary search to find the optimal frequency f_c^* , reducing the complexity of exhaustive search to:

$$O\left(\frac{Q_{max} - 1}{\theta^2} \log_2\left(\frac{f_{c,max} - f_{c,min}}{\theta}\right)\right). \quad (31)$$

It is possible that some values of the parameters does not satisfy the constraints. There are implicit constraints that are not highlighted in problem (P3) but are useful to understand the optimization problem. For example, we can see that from (30) and the upper bound on the compression ratio Q_{max} , that there is a maximum value for α . If we compress with the highest possible compression ratio, we obtain the minimum possible number of packets N^* : these packets must be transmitted, as transmitting fewer packets would lead to a failure in all cases. Specifically, α_{max} is obtained as:

$$\alpha_{max} = 1 - \left\lceil \frac{D}{Q_{max} n_p} \right\rceil \frac{t_p}{T}. \quad (32)$$

This allows to set the limits on the parameters space. The optimization procedure searches parameters combinations within these limits. The non-convexity of this problem and the relationship between the three optimization parameters are analyzed in the following section.

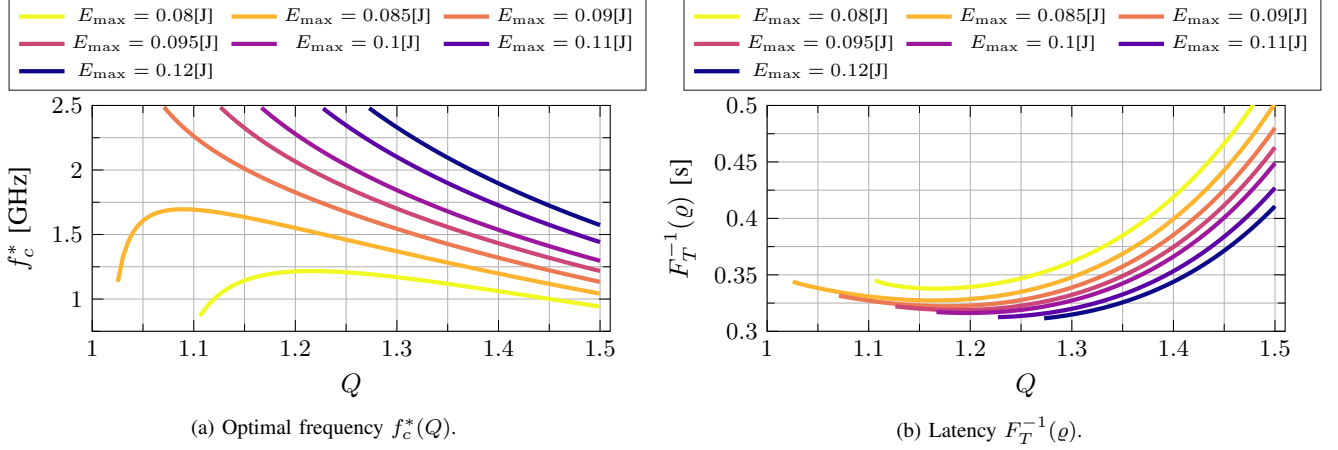


Fig. 3. Optimal frequency and latency of the unconstrained problem (P2) for different values of the maximum energy E_{\max} and $\varrho = 0.9$.

TABLE I
PARAMETERS USED IN THE SIMULATION.

Parameter	Value	Parameter	Value
D	0.5 [Mbit]	d	1000 [m]
κ	1.25	ℓ	2
λ	10^{-15} [J/bit]	N_0	-110 [dBm/Hz]
ν	10^{-14} [J]	ε	0.001
ψ	3.5	K_0	-27 [dB]
P_{tx}	[0.05, 1.5] [W]	f_c	[0.8, 2.5] [GHz]
B	100 [MHz]	ζ	0.05

V. RESULTS

In this section we present some results obtained in the two target scenarios to gain insight into the interplay between communication and computation in terms of energy consumption, latency and reliability. We report the system parameters in Table I, while the channel model and lossless compression ratio interval are taken from [9]. For energy consumption parameters and CPU specifications, we refer to [4]. Reproducible code for the results is provided².

A. Power-Constrained Scenario

In this scenario, we fix the maximum available energy E_{\max} and compute the Pareto front, i.e., the combination of other parameters (Q and f_c) that minimize the latency ϱ -quantile while satisfying the energy constraint. The analysis is repeated for progressively larger values of the energy constraint E_{\max} to explore how the latency quantile evolves as more power becomes available.

To this end, we first illustrate the relationship between the optimal CPU frequency f_c^* and Q , as established in Lemma 1, which reduces problem (P1) to a single-variable optimization in Q . Fig. 3a illustrates the Pareto fronts for different values of E_{\max} , showing the optimal CPU frequency f_c^* as a function of the compression ratio Q for each energy constraint. It is interesting to observe that the f_c^* versus Q curve is concave for smaller values of the energy budget, and convex for larger values. This change is due to the different rate at which the

numerator and denominator of f_c^* in (20) change with Q . For small energy budgets, the numerator of (20) rises quickly at first, while the denominator grows slowly; this makes the ratio, and thus the optimal frequency, increase initially. As the numerator's growth tapers off and the denominator's exponential growth accelerates, the ratio decreases. For large energy budgets, the numerator is almost constant, so the exponentially increasing denominator drives a steady, convex decline in the ratio. Note that for certain values of Q , a feasible solution for f_c^* may not exist. This infeasibility stems from hardware constraints on compression: the energy required for compression depends on the CPU's operating frequency and power consumption, both of which are bounded by physical limits. In practice, processors cannot operate below a minimum frequency $f_{c,\min}$ nor above a maximum frequency $f_{c,\max}$ due to design and thermal constraints. Consequently, we restrict the feasible range to $800 \text{ MHz} \leq f_c^* \leq 2.5 \text{ GHz}$, which reflects realistic hardware capabilities [35].

Next, in Fig. 3b we report the latency ϱ -quantile, denoted by the inverse CDF F_T^{-1} . This corresponds to the minimal latency that still satisfies the reliability requirement ϱ and is obtained using the same (f_c^*, Q) parameter pairs that generate the Pareto fronts in Fig. 3a. We observe that the latency profiles turn out to be convex, thus indicating that for each E_{\max} , there exists a compression ratio Q that minimizes the latency quantile. Comparing the two figures, i.e. Fig. 3a and Fig. 3b, a general trend emerges: as the available energy E_{\max} increases, the optimal operating frequency f_c^* also increases, leading to a reduction in system latency. This confirms the intuition that higher energy budgets enable faster processing and more efficient compression, thereby improving overall performance.

Finally, Fig. 4 illustrates the Pareto front in terms of Energy and Latency ϱ -quantile. Higher ϱ values correspond to progressively stricter maximum-latency guarantees, revealing how tightening reliability requirements reshapes the achievable trade-off. A Pareto front for a given latency quantile or reliability level ϱ is obtained by computing, for each energy constraint, the minimum achievable latency. Equivalently, each point on the front corresponds to a unique combination of CPU frequency f_c and compression ratio Q . For compar-

²<https://github.com/pietro-talli/energy-qaoi-cc>

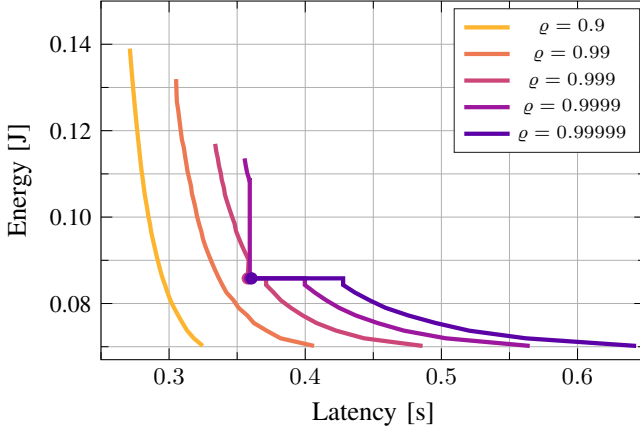


Fig. 4. Pareto front for the power-constrained scenario.

ison, the system's baseline configuration, operating without compression, is marked by a colored dot whenever it lies on the front. The results show that, at lower reliability levels, the joint optimization of f_c and Q consistently yields Pareto-superior configurations compared to the uncompressed baseline. In this regime, compression reduces the data volume to be transmitted, lowering both energy consumption and total latency without incurring a significant penalty from variability in transmission times. The steepness of the Pareto curves in this region highlights that substantial energy savings can be achieved with only marginal increases in latency, underscoring the benefits of jointly optimizing compression and communication parameters when energy budgets are limited. At higher reliability levels, however, reducing the available energy budget causes latency to increase significantly after a certain point. This is because the additional processing time required for compression becomes more significant, particularly in the worst-case tail of the latency distribution. In this setting, we find that the minimum achievable latency, obtained without compression, can be matched at an equal or a lower overall energy budget than with compression, making transmission without compression the more favorable choice.

B. Time-Constrained Scenario

In the time-constrained scenario, we fix the value of T (or equivalently the QAOI) and determine the corresponding Pareto front, representing the set of (f_c, Q) combinations that minimize the total energy consumed in both compression and communication, while satisfying the overall reliability requirement. In this setting, the three optimization variables; the compression/transmission allocation factor α , the CPU frequency f_c , and the compression ratio Q ; are tightly coupled and not explicitly separable. To provide deeper insight into their individual roles and mutual dependencies, we first present a series of plots that illustrate how variations in these parameters influence both the objective function and the overall reliability constraint in problem (P3). Specifically, we examine how the overall reliability or success probability, $P_{\text{succ}} = (1 - \varepsilon_c)(1 - \varepsilon_{\text{tx}})$, and the total energy consumption, $E_c + E_{\text{tx}}$, vary with respect to each optimization variable,

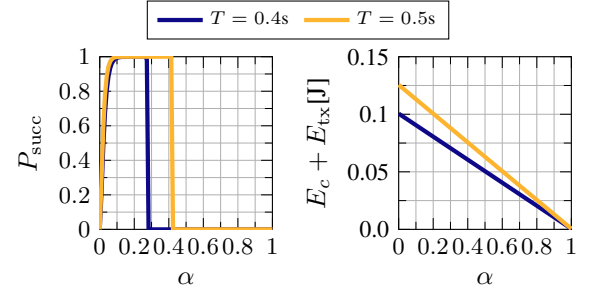


Fig. 5. Overall success probability and total energy consumption for different values of α , $Q = 1.2$ and $f_c = 1.6$ [GHz].

while keeping the other two fixed. In each plot, the two curves correspond to different values of T , thereby highlighting the sensitivity of system performance to QAOI constraints.

We begin with Fig. 5, which examines the influence of α , the fraction of the available time slot allocated to compression. The left plot shows the value of P_{succ} for fixed Q and f_c with varying α . For very small values of α , the communication phase dominates the time allocation, leaving insufficient time for compression. In this regime, the compression success probability $(1 - \varepsilon_c)$ is significantly low, driving the overall reliability toward zero. As α increases, both compression and transmission phases receive adequate time, and the success probabilities improve. The product of the two probabilities approaches one, indicating high overall reliability. However, beyond a certain threshold, allocating more time to compression reduces the time available for transmission, sharply decreasing $(1 - \varepsilon_{\text{tx}})$, and, consequently, the overall reliability drops again toward zero. Furthermore, increasing T from 0.4 to 0.5 broadens the feasible range of α (for fixed f_c and Q) over which the success probability remains high.

In terms of energy, only the transmission energy E_{tx} varies with α , since compression energy is independent of the time allocation for fixed values of f_c and Q (provided that it is completed within the allocated slot). As shown in the right plot of Fig. 5, the total energy consumption exhibits an inverse dependence on α . For small α , insufficient compression time reduces compression success probability, leaving more bits to be transmitted, which drives transmission energy E_{tx} high. As α increases, more bits are successfully compressed, easing the transmission burden and lowering E_{tx} . Beyond a certain

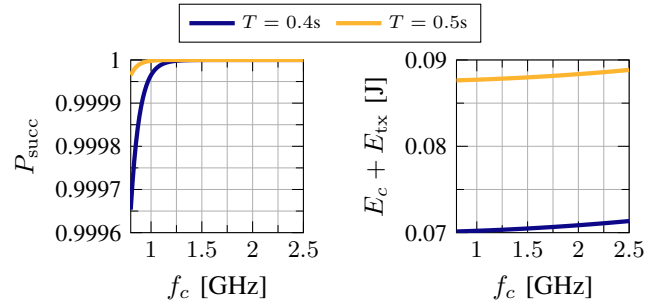


Fig. 6. Overall success probability and total energy consumption for different values of f_c , $Q = 1.2$ and $\alpha = 0.3$.

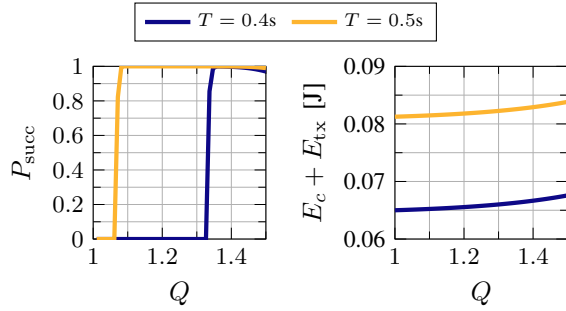


Fig. 7. Overall success probability and total energy consumption for different values of Q , $f_c = 1.6$ [GHz] and $\alpha = 0.35$.

threshold, however, the available transmission time $(1 - \alpha)T$ becomes too short to deliver the compressed payload. In this regime, the transmission energy contribution effectively vanishes, and the total energy drops toward the compression cost alone, which in this case is negligibly low for the given Q and f_c . At last, it is interesting to note that in this scenario increasing T leads to higher overall energy consumption. This is because the communication slot is fully utilized to maximize reliability; without joint optimization, a larger T simply results in more transmissions and hence greater energy usage. This highlights that relaxing T alone does not suffice to reduce energy usage in such time-constrained scenario; true energy minimization requires joint optimization of both compression and communication parameters.

Next, Fig. 6 illustrates the impact of CPU frequency f_c on system performance, showing both the success probability and total energy consumption. As expected, increasing f_c enhances the probability of completing compression within the allocated time, but also increases energy consumption due to the superlinear dependence of computational energy on clock frequency. Moreover, for fixed α and Q , a larger T directly translates into a longer available compression slot αT , which improves the likelihood of completing compression successfully and thus raises the overall success probability. By contrast, the transmission energy E_{tx} remains constant with respect to f_c and dominates the compression energy E_c , especially for larger T . Nevertheless, the monotonic behavior of P_{succ} and $E_c + E_{tx}$ shown in Fig. 6 confirms the existence of an optimal operating point f_c^* that satisfies the reliability constraint with equality, as discussed in Section IV-B.

Fig. 7 illustrates the effect of the compression ratio Q on system performance for fixed $\alpha = 0.35$ and $f_c = 1.6$ [GHz]. When Q is very low, the compression is insufficient to reduce the data load for transmission, so the transmission success probability $(1 - \varepsilon_{tx})$, and consequently P_{succ} , remains near zero. As Q increases, enough redundancy is removed to allow reliable transmission within the available transmission slot, and P_{succ} rises sharply. When Q becomes too large, however, the compression operation itself becomes more complex and time-consuming, lowering the compression success probability $(1 - \varepsilon_c)$ and reducing P_{succ} again. This interaction produces the characteristic rectified-S shape of the curve.

The role of T is also evident: with $T = 0.4$ s, the reliability threshold ϱ is exceeded only when $Q \gtrsim 1.31$. Relaxing T

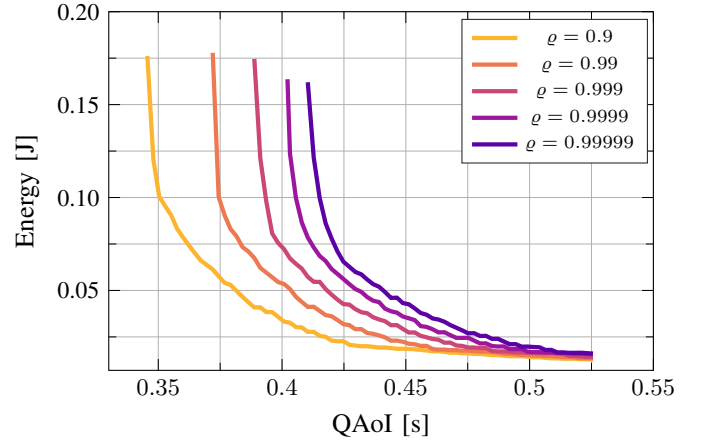


Fig. 8. Pareto front for the time-constrained scenario.

increases the available transmission time, thereby enabling successful transmission even for lower Q . As a consequence, with $T = 0.5$ s, the feasible range of Q that satisfies the reliability constraint broadens significantly. In terms of energy, only the compression energy E_{comp} depends on Q , and it grows superlinearly with Q due to the rising computational cost of stronger compression. Thus, energy consumption increases monotonically with Q , even in the regime where P_{succ} is maximized. As in Fig. 5, increasing T alone does not reduce energy consumption: while a larger T broadens the feasible range of Q values that ensure reliability, true energy minimization requires joint optimization of Q together with the other system parameters. Finally, Fig. 8 presents the Pareto front in terms of total energy consumption and QAoI for different reliability levels ϱ . Each curve is obtained by finding, for a fixed ϱ , the minimum total energy achievable across all feasible configurations. Equivalently, each point on the front represents an optimal pairing of CPU frequency f_c , compression ratio Q and α that meets both the QAoI and reliability requirements. Across all reliability levels, relaxing T , or equivalently the QAoI target, yields a substantial reduction in the total energy required.

This demonstrates the effectiveness of jointly optimizing compression and communication: by slightly loosening freshness constraints, the system can operate at lower frequencies and/or adopt higher compression ratios, thereby reducing both computational and transmission energy demands. The energy savings are especially pronounced in the low-QAoI region of each Pareto curve, where modest concessions in freshness deliver significantly large improvements in overall EE. The trends shown in Fig. 8 broadly mirror those observed in the power-constrained case (Fig. 4), yet key distinctions emerge from the time-constrained setting. Here, the strict separation between compression and communication phases imposes tighter timing constraints to satisfy a given reliability target ϱ , which often necessitates operating over a longer time interval compared to the power-constrained configuration. Irrespective, the joint compression–communication paradigm in the time-constrained scenario can achieve markedly lower total energy

consumption, making it particularly attractive for systems that must uphold stringent reliability while aggressively optimizing for the overall EE.

VI. CONCLUSION

This work demonstrated that substantial energy savings in wireless communication systems can be achieved by relaxing strict latency and reliability constraints, without compromising overall system performance. Using a cross-layer optimization approach, we systematically explored the trade-offs between data compression, latency, and energy consumption. Our analysis considered two representative scenarios: power-constrained systems and time-constrained systems, each reflecting practical deployment contexts such as battery-limited sensor nodes or systems with strict scheduling requirements. Through a detailed end-to-end formulation for both scenarios, we provided a comprehensive view of how system parameters, including CPU frequency, compression ratio, and time allocation, can be jointly tuned to minimize energy consumption while meeting application-specific requirements for data freshness and delivery success. In the power-constrained case, we focused on latency as the key performance metric. In the time-constrained case, we used QoI as a meaningful metric to capture both temporal relevance and reliability under variable compression and transmission dynamics. Simulation results validated the analytical findings and underscored the practical relevance of our framework. In particular, they showed that modest relaxations in reliability and latency requirements can enable significant reductions in energy use, which is a critical outcome for battery-powered or energy-harvesting systems operating under long-term deployment constraints.

Looking ahead, future work could extend this framework by incorporating lossy compression schemes and adopting a value-of-information (VoI) perspective, where the utility of the reported data depends not only on its freshness but also on the distortion introduced by compression and reconstruction. Such an approach would enable adaptive and application-aware communication strategies, where resources are allocated based on the perceived importance or informativeness of the transmitted data. Additional research may also explore real-time adaptation mechanisms, multi-hop extensions, and learning-based optimization techniques to further enhance the scalability and robustness of the proposed models in dynamic network environments.

REFERENCES

- [1] M. Marjani *et al.*, “Big IoT data analytics: architecture, opportunities, and open research challenges,” *IEEE Access*, vol. 5, pp. 5247–5261, 2017.
- [2] J. Yick, B. Mukherjee, and D. Ghosal, “Wireless sensor network survey,” *Computer Networks*, vol. 52, no. 12, pp. 2292–2330, 2008.
- [3] B. Varghese *et al.*, “A survey on edge performance benchmarking,” *ACM Computing Surveys (CSUR)*, vol. 54, no. 3, pp. 1–33, 2021.
- [4] I. Leyva-Mayorga *et al.*, “Satellite edge computing for real-time and very-high resolution earth observation,” *IEEE Transactions on Communications*, vol. 71, no. 10, pp. 6180–6194, 2023.
- [5] J. Shao and J. Zhang, “Communication-computation trade-off in resource-constrained edge inference,” *IEEE Communications Magazine*, vol. 58, no. 12, pp. 20–26, 2020.
- [6] Y. Chen, S. Zhang, S. Xu, and G. Y. Li, “Fundamental trade-offs on green wireless networks,” *IEEE Communications Magazine*, vol. 49, no. 6, pp. 30–37, 2011.
- [7] K. C. Barr and K. Asanović, “Energy-aware lossless data compression,” *ACM Trans. Comput. Syst.*, vol. 24, no. 3, p. 250–291, Aug. 2006. [Online]. Available: <https://doi.org/10.1145/1151690.1151692>
- [8] A. Avranas, M. Kountouris, and P. Ciblat, “Energy-latency tradeoff in ultra-reliable low-latency communication with retransmissions,” *IEEE Journal on Selected Areas in Communications*, vol. 36, no. 11, pp. 2475–2485, 2018.
- [9] S. Suman *et al.*, “Statistical characterization of closed-loop latency at the mobile edge,” *IEEE Transactions on Communications*, vol. 71, no. 7, pp. 4391–4405, 2023.
- [10] L. Li, A. E. Kalør, P. Popovski, and W. Chen, “Unified timing analysis for closed-loop goal-oriented wireless communication,” *IEEE Transactions on Wireless Communications*, 2025.
- [11] F. Chiarriotti *et al.*, “Query age of information: Freshness in pull-based communication,” *IEEE Transactions on Communications*, vol. 70, no. 3, pp. 1606–1622, 2022.
- [12] B. Hochwald and K. Zeger, “Tradeoff between source and channel coding,” *IEEE Transactions on Information Theory*, vol. 43, no. 5, pp. 1412–1424, 1997.
- [13] J. Hagenauer, “Source-controlled channel decoding,” *IEEE Transactions on Communications*, vol. 43, no. 9, pp. 2449–2457, 1995.
- [14] R. Berry and R. Gallager, “Communication over fading channels with delay constraints,” *IEEE Transactions on Information Theory*, vol. 48, no. 5, pp. 1135–1149, 2002.
- [15] M. U. Baig, L. Yu, Z. Xiong, A. Høst-Madsen, H. Li, and W. Li, “On the energy-delay tradeoff in streaming data: Finite blocklength analysis,” *IEEE Transactions on Information Theory*, vol. 66, no. 3, pp. 1861–1881, 2020.
- [16] T. D. Burd and R. W. Brodersen, “Processor design for portable systems,” *Journal of VLSI signal processing systems for signal, image and video technology*, vol. 13, no. 2, pp. 203–221, 1996.
- [17] K. De Vogeleer, G. Memmi, P. Jouvelot, and F. Coelho, “The energy/frequency convexity rule: Modeling and experimental validation on mobile devices,” in *International Conference on Parallel Processing and Applied Mathematics*. Springer, 2013, pp. 793–803.
- [18] Y. Mao *et al.*, “A survey on mobile edge computing: The communication perspective,” *IEEE communications surveys & tutorials*, vol. 19, no. 4, pp. 2322–2358, 2017.
- [19] S. Li, M. A. Maddah-Ali, Q. Yu, and A. S. Avestimehr, “A fundamental tradeoff between computation and communication in distributed computing,” *IEEE Transactions on Information Theory*, vol. 64, no. 1, pp. 109–128, 2017.
- [20] L. Ballotta, L. Schenato, and L. Carlone, “Computation-communication trade-offs and sensor selection in real-time estimation for processing networks,” *IEEE Transactions on Network Science and Engineering*, vol. 7, no. 4, pp. 2952–2965, 2020.
- [21] P. Popovski, F. Chiarriotti, K. Huang, A. E. Kalør, M. Kountouris, N. Pappas, and B. Soret, “A perspective on time toward wireless 6g,” *Proceedings of the IEEE*, vol. 110, no. 8, pp. 1116–1146, 2022.
- [22] J. Ziv and A. Lempel, “A universal algorithm for sequential data compression,” *IEEE Transactions on information theory*, vol. 23, no. 3, pp. 337–343, May 1977.
- [23] X. Li *et al.*, “Wirelessly powered crowd sensing: Joint power transfer, sensing, compression, and transmission,” *IEEE Journal on Selected Areas in Communications*, vol. 37, no. 2, pp. 391–406, 2018.
- [24] S. Jošilo and G. Dán, “Selfish decentralized computation offloading for mobile cloud computing in dense wireless networks,” *IEEE Transactions on Mobile Computing*, vol. 18, no. 1, pp. 207–220, 2018.
- [25] D. Han *et al.*, “Offloading optimization and bottleneck analysis for mobile cloud computing,” *IEEE Transactions on Communications*, vol. 67, no. 9, pp. 6153–6167, 2019.
- [26] J.-B. Wang *et al.*, “Joint optimization of transmission bandwidth allocation and data compression for mobile-edge computing systems,” *IEEE Communications Letters*, vol. 24, no. 10, pp. 2245–2249, 2020.
- [27] R. Kothiyal *et al.*, “Energy and performance evaluation of lossless file data compression on server systems,” in *SYSTOR*, 2009.
- [28] M. Burrows *et al.*, “On-line data compression in a log-structured file system,” *ACM SIGPLAN Notices*, vol. 27, no. 9, pp. 2–9, 1992.
- [29] Z. Zhang *et al.*, “Efficient I/O for neural network training with compressed data,” in *2020 IEEE International Parallel and Distributed Processing Symposium (IPDPS)*. IEEE, 2020, pp. 409–418.
- [30] D. Tse and P. Viswanath, *Fundamentals of wireless communication*. Cambridge university press, 2005.

- [31] E. Björnson and E. G. Larsson, “How energy-efficient can a wireless communication system become?” in *2018 52nd Asilomar conference on signals, systems, and computers*. IEEE, 2018, pp. 1252–1256.
- [32] M. Bagnoli and T. Bergstrom, “Log-concave probability and its applications,” in *Rationality and Equilibrium: A Symposium in Honor of Marcel K. Richter*. Springer, 2006, pp. 217–241.
- [33] L. Rizzo, “Effective erasure codes for reliable computer communication protocols,” *ACM SIGCOMM computer communication review*, vol. 27, no. 2, p. 24–36, 1997.
- [34] D. H. Alai, Z. Landsman, and M. Sherris, “Lifetime dependence modelling using a truncated multivariate gamma distribution,” *Insurance: Mathematics and Economics*, vol. 52, no. 3, pp. 542–549, 2013.
- [35] M. Capra, R. Peloso, G. Masera, M. Ruoch, and M. Martina, “Edge computing: A survey on the hardware requirements in the internet of things world,” *Future Internet*, vol. 11, no. 4, p. 100, 2019.

APPENDIX A

CONVEXITY OF THE COMPRESSION LATENCY QUANTILE

We now prove that the quantile of the Gamma distribution representing the compression latency is convex under the condition in (22). It is known that the ϱ -quantile of the Gamma distribution of parameters (α, β) can be expressed as

$$\gamma^{-1}(\alpha, \Gamma(\alpha)\varrho) \cdot \beta, \quad (33)$$

where γ and Γ are the lower incomplete Gamma function and the Gamma function, respectively. In our case, β is the only parameter that depends on Q , through the relation

$$\beta = \frac{e^{\psi Q} - e^{\psi}}{\kappa f_c^*(Q)} = K \sqrt{\frac{(e^{\psi Q} - e^{\psi})^3}{E_{\max} - \frac{C}{Q}}}, \quad (34)$$

where K and $C = \frac{D}{(1-\varepsilon)\eta(\varepsilon)}$ are positive constants which do not depend on Q . We are left to show that β is convex with respect to Q . To this end, we analyze the sign of the second order derivative of (34) with respect to Q , which is equal to

$$\begin{aligned} \frac{d^2\beta(Q)}{dQ^2} = \frac{1}{2}K\beta(Q) & \left\{ \frac{1}{2} \left[\frac{C}{Q(QE_{\max} - C)} - \frac{3\psi e^{\psi Q}}{e^{\psi Q} - e^{\psi}} \right]^2 \right. \\ & \left. + \frac{3\psi^2 e^{\psi} e^{\psi Q}}{(e^{\psi Q} - e^{\psi})^2} + \frac{-2QE_{\max} + C}{Q^2 E_{\max} - CQ} \right\}. \end{aligned} \quad (35)$$

This function is positive (and, hence, β is convex in Q), if

$$\frac{3\psi^2 e^{\psi} e^{\psi Q}}{(e^{\psi Q} - e^{\psi})^2} + \frac{-2QE_{\max} + C}{Q^2 E_{\max} - CQ} \geq 0, \quad (36)$$

as all the other terms are non-negative. However, showing that the condition (36) is satisfied is not trivial, as the first two terms have opposite signs. We then give

$$f_c^* = \sqrt{\frac{f_{\max}^3}{DP_{s,\max}} \frac{E_{\max} - \frac{C}{Q}}{e^{\psi Q} - e^{\psi}}} \quad (37)$$

$$e^{\psi Q} = e^{\psi} + \frac{f_{\max}^3}{f_c^{*2} DP_{s,\max}} \left(E_{\max} - \frac{C}{Q} \right) \quad (38)$$

$$Q = \psi^{-1} \log \left[\frac{f_{\max}^3}{f_c^{*2} DP_{s,\max}} \left(E_{\max} - \frac{C}{Q} \right) + e^{\psi} \right]. \quad (39)$$

Substituting (38) and (39) into the first term of (36) and further simplifying, we obtain the final condition

$$Q^2 3\psi^2 e^{\psi} - 2QE_{\max} + C \geq 0, \quad (40)$$

which is the condition in the theorem statement.